Range/velocity limitations for time-domain blood velocity estimation

Jensen, Jørgen Arendt

Published in:
Ultrasound in Medicine & Biology

Publication date:
1993

Document Version
Publisher's PDF, also known as Version of record

Ultrasound in Med. & Biol. Vol. 19, No. 9, pp. 741–749, 1993
Printed in the USA

0301-5629/93 $6.00 + .00

●*Original Contribution*

RANGE/VELOCITY LIMITATIONS FOR TIME-DOMAIN BLOOD VELOCITY ESTIMATION

JØRGEN ARENDT JENSEN
Bioacoustics Research Laboratory, Department of Electrical and Computer Engineering, University of Illinois at Urbana-Champaign, 1406 West Green Street, Urbana, IL 61801-2991, USA

(*Received* 24 *February* 1993; *in final form* 22 *July* 1993)

Abstract—The traditional range/velocity limitation for blood velocity estimation systems using ultrasound is elucidated. It is stated that the equation is a property of the estimator used, not the actual physical measurement situation, as higher velocities can be estimated by the time domain cross-correlation approach. It is demonstrated that the time domain technique under certain measurement conditions will yield unsatisfactory results, when trying to estimate high velocities. Various methods to avoid these artifacts using temporal and spatial clustering techniques are suggested. The improvement in probability of correct detection is derived, and several examples of simulations are shown.

Key Words: **Velocity estimation, Medical ultrasound, Range/velocity limitation.**

INTRODUCTION

The 1980s saw the introduction of ultrasound systems capable of both estimating blood velocity and displaying the information in real time as a color flow map. These systems provide the clinical community with a tool for rapid and inexpensive investigation of the human circulatory system. This has made it possible to investigate, for example, circulation in lower limbs, arterial stenosis and cardiovascular deficiencies, among numerous other diagnostic applications.

Although they are very useful tools, there are still major restrictions enforced on the quantities that can be measured by these systems. Most notably, the velocity measurement is angle dependent, and only velocity components towards or away from the transducer are detected. Further, limits exist on the maximum velocity detectable. The last restriction stems from the depth-velocity limitation, which gives the relation between the maximum velocity that can be uniquely determined and depth in tissue. When a too large velocity is present, it will be aliased and presented as, *e.g.*, a negative velocity, causing confusion between a high velocity stream and a turbulent stream.

Many clinical situations exist where this can create problems. These cases include the study of high velocity jets in stenosed vessels, valvular defects and distinguishing between high velocity jets from intraventricular obstruction and that of the associated mitral regurgitation (Hatle and Angelsen 1982). Thus, there are many reasons for trying to construct systems with a less restricted range of detectable velocities.

Address correspondence to: Jørgen Arendt Jensen.

TRADITIONAL RANGE/VELOCITY LIMITATION

Most current blood velocity estimation systems are based on the autocorrelation approach suggested by Namekawa et al. (1982) and further described in Kasai et al. (1985). The method detects the movement of blood scatterers in the time elapsed between reception of consecutive pulse-echo lines. The velocity is estimated from the phase shift between the lines as:

$$\hat{v}_z = \frac{c}{2\pi f_0 2T_{prf}} \hat{\phi}_v, \tag{1}$$

where f_0 is the transducer center frequency, c is the propagation velocity, and T_{prf} is the time between pulse emissions. $\hat{\phi}_v$ is the estimated phase shift usually found from the complex autocorrelation between the lines. This phase shift can only be uniquely determined between $-\pi$ and π, limiting the largest detectable velocity to:

$$\hat{v}_{\max} = \frac{c}{2\pi f_0 2T_{prf}}\pi = \frac{c}{4}\frac{1}{f_0 T_{prf}}. \quad (2)$$

The largest depth into the body that can be investigated uniquely, is limited by the pulse repetition time and the propagation velocity, so:

$$2d_{\max} < cT_{prf}. \quad (3)$$

Combining this with (2) yields the depth/velocity limitation for phase shift measurement systems:

$$v_{\max} = \frac{c^2}{8d_{\max} f_0}. \quad (4)$$

This has been characterized by some as a basic, physical limitation for ultrasound systems estimating blood velocity. It is not. It is merely a limitation of the estimator used, because it makes use of a phase shift. It is possible to find the shift in position of the scatterers, when they move between pulses by more than half a wavelength in the beam direction. A technique for doing that using cross-correlation has been suggested by a number of authors (Dotti et al. 1976; Bonnefous et al. 1986; Foster et al. 1990). In this method the high frequency transducer signal is sampled following consecutive transmitted pulses. Small segments of data, at the same depth in tissue, are extracted from each line and cross-correlated. The position of the maximum in the cross-correlation function then indicates the shift in time t_s between the echoes, due to the movement of the blood scatterers. It is related to the velocity by:

$$\hat{v}_z = \frac{c}{2}\frac{t_s}{T_{prf}}. \quad (5)$$

The method has no inherent limitation in maximum detectable velocity apart from that set by the distance over which the two received signals are correlated. Dependent on the actual flow and the composition of the blood, the maximum velocity might be several times larger than $v_{\max}$ in (2).

PROBABILITY OF CORRECT DETECTION

The estimation of the velocity by the time-domain technique is done by finding the position of the maximum in the cross-correlation function. The reliability of this nonlinear approach depends on the quality of the estimated cross-correlation function. An example is shown in Fig. 1. Due to noise in the acquired signals and the use of a limited amount of data, it is quite possible that the maximum will be at a position different from that which the true velocity would indicate. That this, indeed, is the case was shown by Jensen (1993a) and Jensen (1993b). Here it was demonstrated that false maxima exist, and that it is appropriate to state a probability of correct estimation. The probability of correct detection is defined here as the

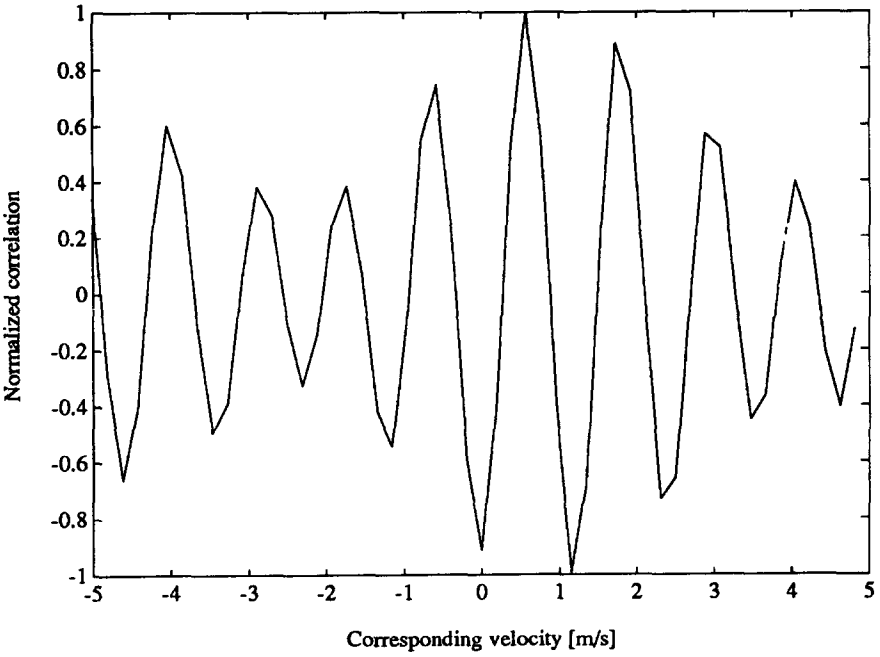

Fig. 1. Cross-correlation function for v = 0.5 m/s.

fraction of estimates that are equal to the true velocity within an interval of ±2.5% of the maximum detectable velocity. The probability is influenced by signal-to-noise ratio, number of pulse-echo lines used, velocity, transducer bandwidth and length of range gate. An example of the distribution of velocity estimates is shown in Fig. 2. The graph is a result from a simulation as described by Jensen (1993b). Four transmitted pulses were used for each estimation and the signal-to-noise ratio was 0 dB. The true velocity was 0.5 m/s. Stationary echo canceling was performed by subtracting consecutive lines. In this case the largest number of estimates is centered around the true velocity surrounded by two smaller peaks. The cross-correlation function is a time shifted version of the autocorrelation function of the interrogating pulse, and the two small peaks in the distribution are located at the first side lobes of the cross-correlation function in Fig. 1. From Fig. 2 it is, thus, seen that there is some probability that peaks outside the main lobe of the cross-correlation are the largest. It should be noted that the estimates are quite narrowly centered around the true velocity, indicating that a small variance can be attained once the correct peak is located.

One possible method for increasing the probability of correct detection is to lower the side lobe peaks in the cross-correlation function. This is attained by selecting a shorter pulse, thus yielding a narrower autocorrelation. The frequency-dependent attenuation will, however, gradually lengthen the pulse, as it propagates through tissue. Using even the shortest pulse will, therefore, still give false detections, and other techniques are needed in order to solve the problem.

LIMITING THE SEARCH RANGE

One possible solution to the false detection problem is to restrict the search for the maximum to lie within the two side lobe peaks. Doing this limits the maximum possible time shift to:

$$t_{\text{smax}} = \frac{1}{f_0}, \tag{6}$$

and the maximum velocity to

$$v_{\max} = \frac{c}{2} \frac{1}{f_0 T_{prf}}. \tag{7}$$

Trying further to avoid the false peaks at the side lobes, the maximum time shift must be only half a period of f_0, limiting the maximum velocity to:

$$v_{\max} = \frac{c}{4} \frac{1}{f_0 T_{prf}}, \tag{8}$$

which is equal to the maximum detectable velocity for the autocorrelation approach.

The influence of limiting the search range is shown in Fig. 3 (dashed lines) along with data for the

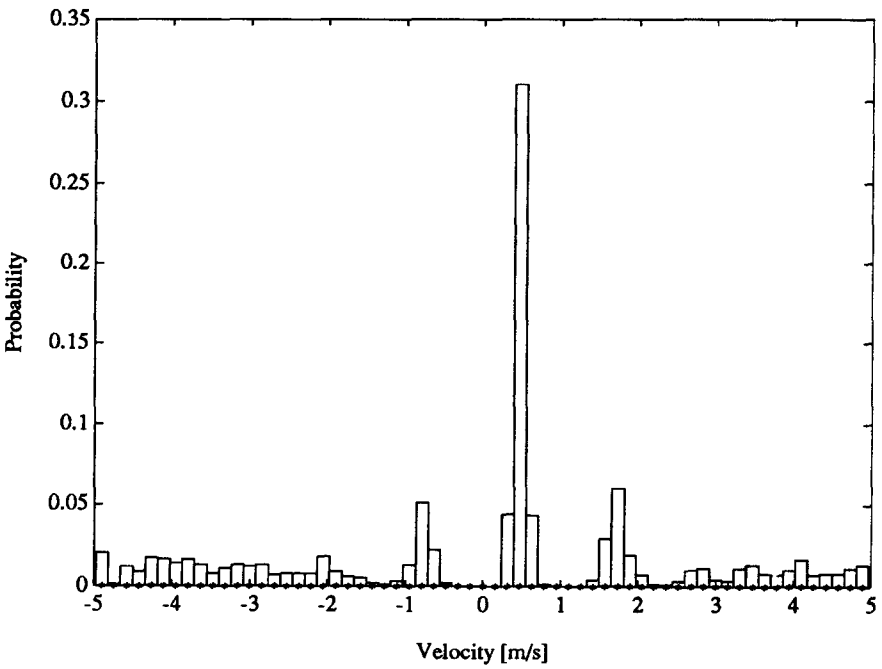

Fig. 2. Distribution of velocity estimates for v = 0.5 m/s.

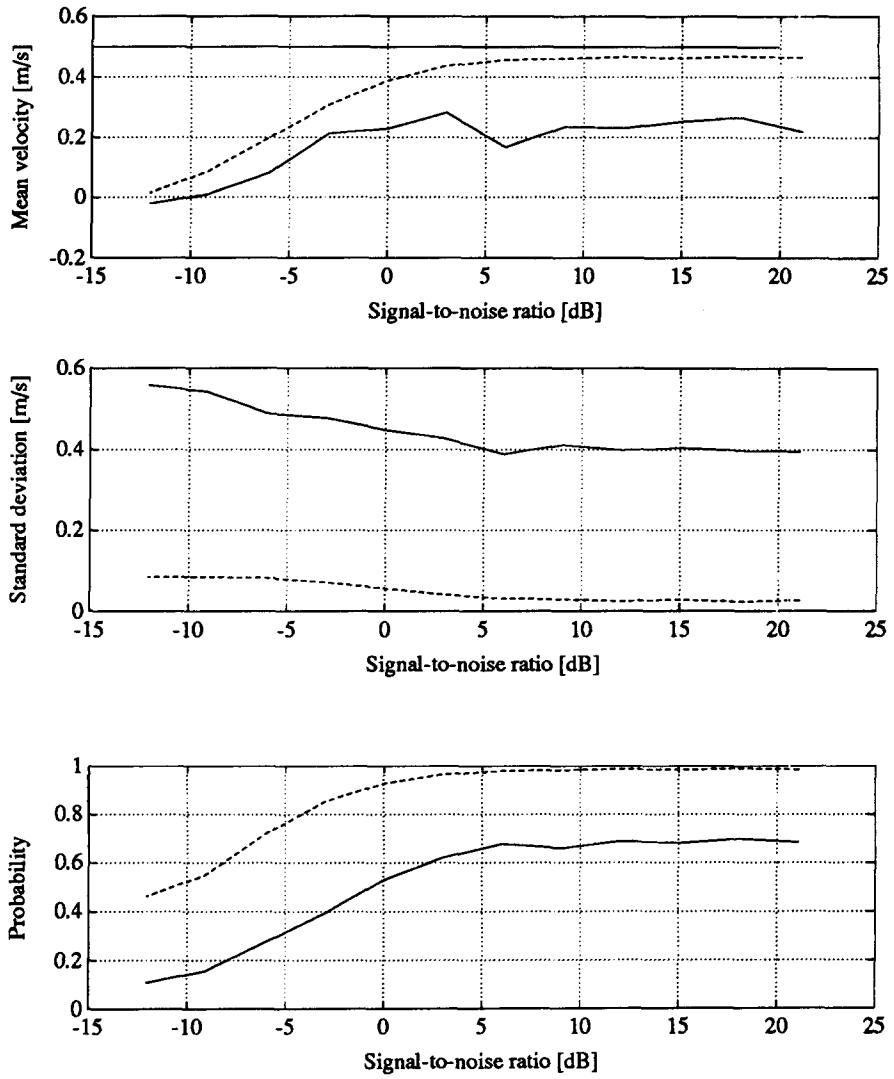

Fig. 3. Mean velocity, standard deviation and probability of correct detection for a velocity of 0.5 m/s. Solid line shows when the full cross-correlation estimate is searched and dashed line shows when only the main lobe is used.

full range search (solid lines). The top graph shows mean velocity obtained from 1000 simulated estimates found at different signal-to-noise ratios. The true velocity is 0.5 m/s, and 4 pulse-echo lines were used with a range gate of 1.33 μs. Stationary echo canceling was performed. The second graph depicts the standard deviation and the third shows the probability of correct detection. The probability value reaches 0.7 for good signal-to-noise ratios, when the full cross-correlation is searched for the maximum. This is due to the segmentation or range gating of the data. The received signal is random, due to the summation from the many small particles in the blood, and it will fluctuate in strength. It is quite probable that some scattering particles entering the volume of investigation will yield a stronger returned signal, and thereby dominate the cross-correlation function, creating an incorrect maximum. This can also be seen to affect the mean value, which is biased, and the standard deviation is prohibitively large. The problem can be solved by searching only the main lobe. The estimates become unbiased above a signal-to-noise ratio of 6 dB, and the standard deviation falls to a low value. Further, the probability gets close to one. The main disadvantage of the approach is the limit on the maximum velocity, which is the same as that for the autocorrelation approach.

All of the problems with regard to bias and a large variance on the estimates can, thus, be traced back to the problem of finding the correct peak. Once found, the estimation scheme yields a good estimate of the correct velocity.

INCREASING THE PROBABILITY OF CORRECT DETECTION

As seen from Fig. 3, the problem is how to restrict the search range to lie around the probable velocity. Several techniques can be devised.

Due to the finite acceleration of the blood flow there will be a temporal correlation between consecutive estimates. One method is, therefore, to restrict the peak search to lie within a band around the previously estimated velocity at the same spatial location. This demands that the acceleration multiplied by the time between estimates is restricted by:

$$a \cdot t_m < v_{\max} = \frac{c}{4} \frac{1}{f_0 T_{prf}}, \tag{9}$$

where a is the acceleration of the blood and t_m is the time between estimates, usually equal to the time between images displayed. For f_0 = 3 MHz and $1/T_{prf}$ = 5 kHz, $a \cdot t_m$ is 0.64 m/s. A frame rate of 10 Hz gives a maximum allowable acceleration of 6.4 m/s^2.

The disadvantage of this scheme is that once a wrong peak is detected it propagates to the next estimate, possibly resulting in a string of wrong estimates. One method for alleviating this problem is to use a number of estimates taken under the same circumstances, and then select the most probable velocity. If the data acquisition is synchronized to the heartbeat, a new estimate can be acquired at the same flow conditions as that found for previous estimates, provided there is no turbulence present and the heartbeat is regular. Combined with $N-1$ previous estimates, the most likely velocity can be found. It is most probable that the maximum will be at either the correct main lobe or at one of the side lobe peaks. The procedure is then to group the time shift estimates into clusters separated by $1/f_0$. This will give the correct velocity if just $N/2 + 1$ estimates are correct. The new probability of correct detection can be expressed by:

$$p_c = \sum_{k=N_1}^{N} \binom{N}{k} p^k (1-p)^{N-k}, \tag{10}$$

where N_1 is equal to the integer larger than $N/2$, p is the probability of correct detection for the individual estimates, and $\binom{N}{k} = \frac{N!}{k!(N-k)!}$. Eqn. (10) is the sum of probabilities of all possible outcomes that will lead to a correct velocity detection. Figure 4 shows the effect on the resulting probability. The ordinate is the original probability of correct detection for the individual estimates, and the abscissa is the probability after processing. The graph shows the probability transfer function, when five estimates are used. Fewer estimates will give a curve closer to a straight line and more estimates yield a curve with a steeper slope around $p = 0.5$. The output of the procedure can be

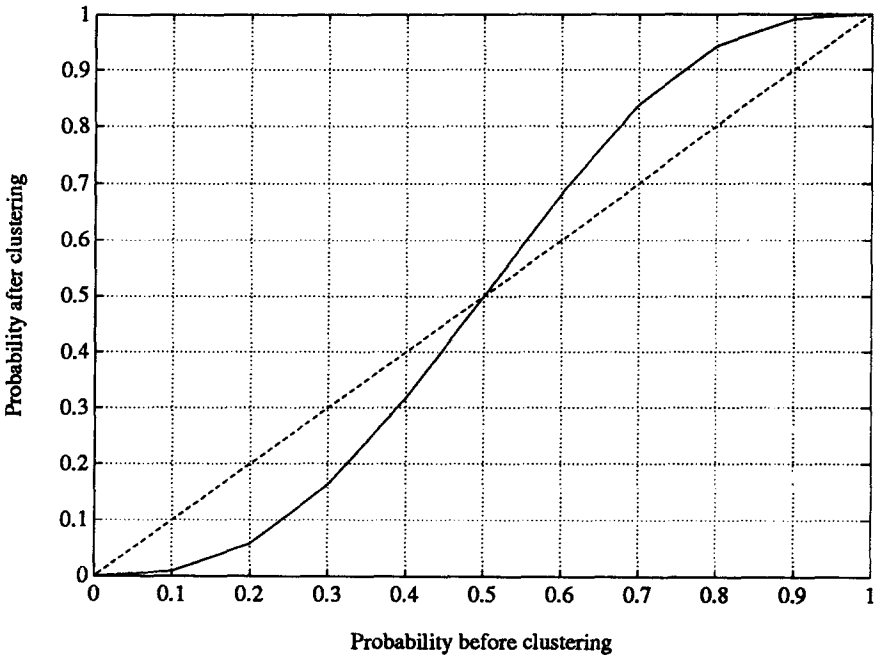

Fig. 4. Probability transfer function for selection technique using five estimates.

the last estimate detected or can be an exponentially weighted average of the last few estimates.

One possible change is to let the processed estimates enter the selection scheme instead of the estimates found directly from the cross-correlation function. This would increase p_c provided that p is larger than 0.5, that initial estimates are correct and that no rapid changes occur in the flow. Using this method, it is advisable to initially use more estimates to increase the initial probability of correct detection. Another way of increasing the probability is to use more pulse-echo lines for calculating the cross-correlation estimates as demonstrated by Jensen (1993a) and Jensen (1993b). This will initially lower the frame rate, but will give a better basis for starting the procedure. A second initial improvement is to use larger range gates, and, thus, increase the integration time used when calculating the cross-correlation. The disadvantage of this is that the assumption of a single velocity within the range gate is less accurate, and that may result in a decreased correlation of the data (Bonnefous 1989) offsetting the advantage of a longer integration time.

A further improvement would be to use knowledge from flow physics. Due to the viscosity of blood, no discontinuities in velocity will be found in a vessel; thus, the velocity profile is a smooth function of spatial coordinates. It is valid to assume that spatially adjacent velocity samples will not have markedly different velocities. Constraints on possible velocities can then be found from the vessels spatial extent and the maximum velocity detected. The velocity at vessel walls should be low and the profile should be a smooth function, again provided there is no flow turbulence.

All of the aforementioned techniques can be incorporated into a time domain cross-correlation flow imaging system. Using advanced pulsing strategies it is possible to selectively enhance velocity estimates at different locations by collecting more lines for certain directions. This could selectively enhance the probability of correct detection.

SIMULATION RESULTS

This section will show some examples of simple one-dimensional simulations of the approaches suggested in the previous section. The pulsatile velocity waveform used is shown in Fig. 5. It was derived from data given by Evans et al. (1989) measured from the femoral artery. A mean velocity waveform was measured here, and the pulsatile velocity profile was calculated using the theory derived by Womersley (1955) and Evans (1982). Using the data from Evans et al. (1989), the velocity waveform at the center of the common femoral artery was found and is shown in Fig. 5. The waveform was calculated from an eighth order Fourier expansion given by:

$$v(t) = 2v_0 + \sum_{k=1}^{8} v_k \cos(k\omega t + \phi_k). \qquad (11)$$

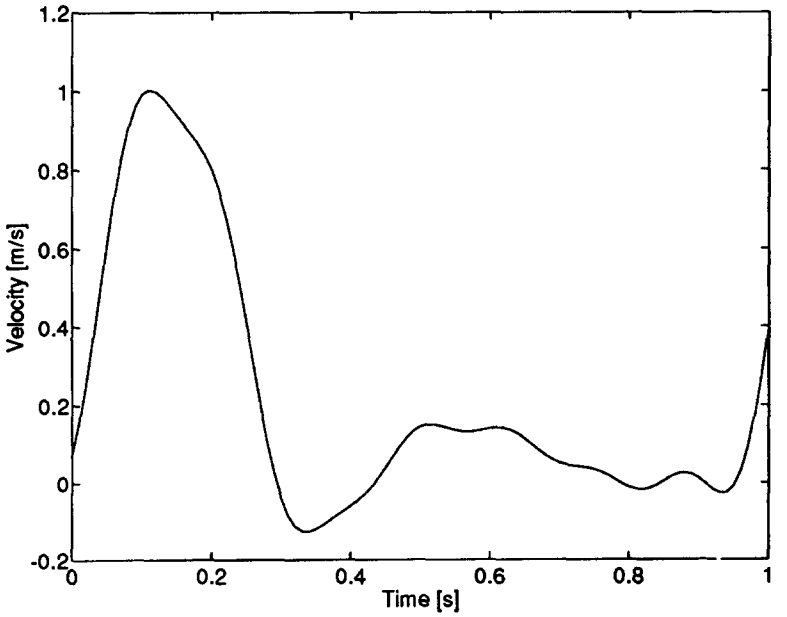

Fig. 5. Example of pulsatile velocity waveform from center of common femoral artery.

The components at the center of the vessel are given in Table 1.

Figure 6 shows different examples of velocity waveforms estimated from simulated data. The data were generated by convoluting a Gaussian pulse with a white, random signal and adding Gaussian, white noise. The center frequency of the pulse was 3 MHz and the relative bandwidth 0.2. The movement of the blood was simulated by translating the responses received relative to the pulse emission in accordance with the blood velocity. One received signal is thus shifted $t_s = \frac{2v_z}{c} T_{prf}$ seconds relative to the previously received signal. A signal-to-noise ratio of 6 dB was used, and four pulses were employed for each estimate. The pulse repetition rate was 5 kHz and the frame rate 10 Hz, so there is 0.1 second between the displayed estimates. The cross-correlation function is calculated by dividing the A-lines received into segments with an equivalent length of four wavelengths, and then correlating with adjacent segments from the previous A-line. No stationary echo canceling was performed.

Results from the simulations are shown in Fig. 6. The solid line indicates the estimated velocity waveform and the circles show the current velocity value. The top graph shows the estimates obtained when the whole cross-correlation function is searched for the maximum. It is quite clear that this is unsuitable for giving an indication of the velocity waveform. The second graph shows the results from limiting the search to the main lobe of the cross-correlation function. The maximum detectable velocity is then $c/4 \cdot f_{prf}/f_0 = 0.64$ m/s, so the maximum velocity in the vessel exceeds this limit. Low velocities are detected correctly, but the peak velocity cannot be correctly estimated.

The third graph shows the estimates when the periodicity of the velocity waveform is used. Estimates from five previous acquisitions taken at the same time relative to the peak in the response is used in the approach mentioned previously in the section on increasing the probability of correct detection. The technique is implemented as follows: the cross-correlation function is divided into segments, each spanning lags equivalent to the main lobe. The mean position of all of the estimates relative to these segments is found. Segments with centers around this mean value are then formed and all the estimates are grouped into these new segments. The number of occurrences of estimates in a segment is counted, and the segment with the highest count is selected as indicating the range of the most probable velocity. The current estimate is then offset to lie within this velocity range. This will increase the probability of correct detection.

A further benefit is that the count of estimates within the selected segment is an indication of how reliable that particular estimate is. A count over 3 indicates a reliable estimate, whereas a count equal to or below 3 should be questioned.

An example of this approach is shown in the third graph in Fig. 6. The instance where less than three estimates were found within the selecting segment is marked in the figure with an × over the symbol O, indicating the true velocity. The procedure can point out the fault in most cases of a wrong detection, although correct detections are also flagged at times. The estimates for low velocities are still not as accurate as for the limited search range, but overall a significant improvement is seen. The scheme has been initialized from acquiring data over 5 pulse beats prior to the data shown in order to get sufficient information to make a detection.

One thing worth noting from Fig. 2 is that once a wrong peak is detected outside the main lobe, there is a nearly rectangular distribution of the probability. This indicates that limiting the search range to, *e.g.*, four times the main lobe would increase the probability. This was done in the fourth graph in Fig. 6. A rather satisfactory result is now obtained, as nearly all estimates are correct even for this low signal-to-noise ratio and using only four A-lines. With these settings 10 images a second can be displayed, each holding 125 lines covering a depth up to 15 cm. Alternatively, more averaging could be done or the frame rate increased.

Table 1. Fourier components of the velocity waveform.

Harmonic k	Frequency Hz	ϕ_k rad	v_k m/s
	0.0	0.0	0.221
1	1.03	−0.886	0.300
2	2.05	−1.713	0.327
3	3.08	−2.883	0.162
4	4.10	−3.504	0.040
5	5.13	−2.443	0.033
6	6.15	−2.816	0.039
7	7.18	−3.506	0.034
8	8.21	−5.506	0.001

CONCLUSION

It has been pointed out that the range/velocity limitation for blood velocity estimation by the conventional autocorrelation approach stems from the use of phase shift estimation. It is, thus, not a physical limitation for this measurement type, but rather a property of the estimator employed. The limitation can in prin-

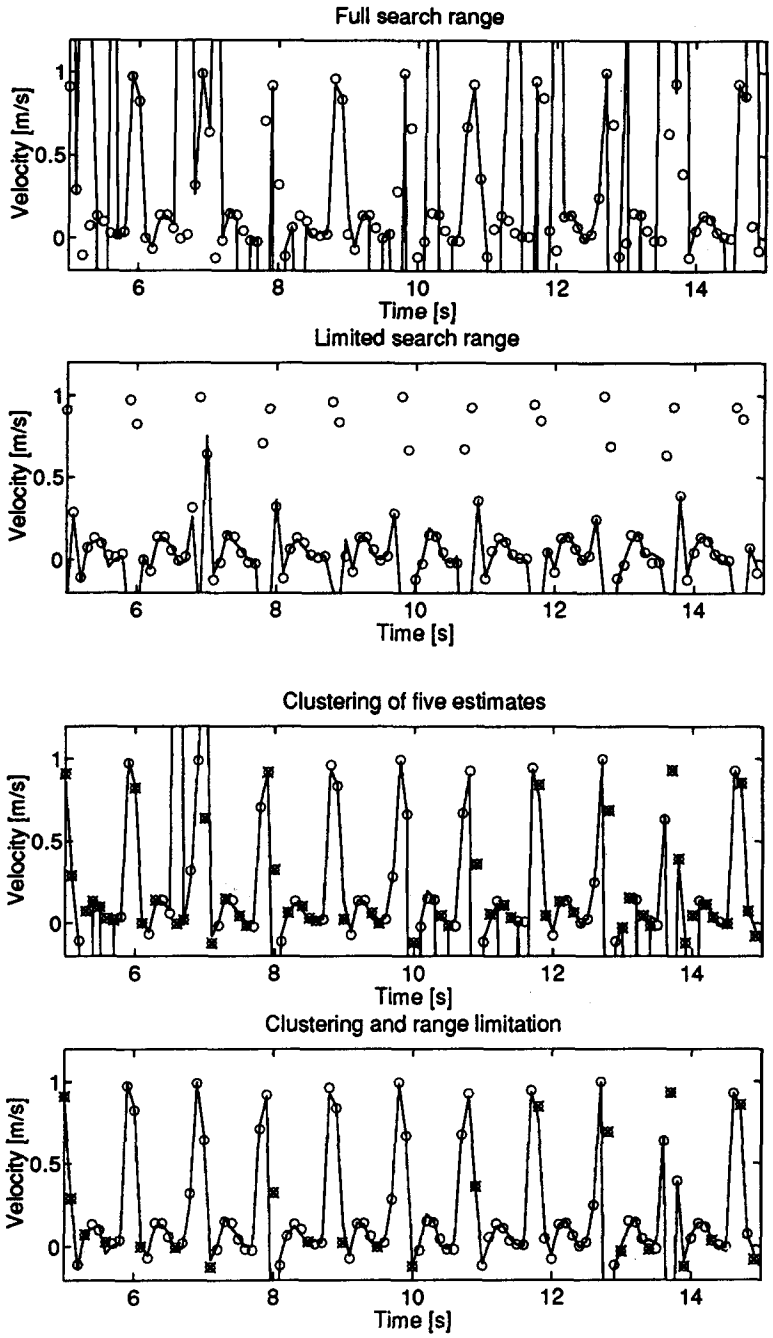

Fig. 6. Estimates of the velocity using the full search range (top) and restricting the range to the main lobe of the cross-correlation (second). Bottom two graphs show wave-forms when a clustering technique is used. The dashed lines depict the estimates and O the actual velocity. × denotes an estimate with a low reliability (see text).

ciple be alleviated by employing the time domain cross-correlation approach. This technique has no inherent limitation in maximum detectable velocity, apart from that set by the range over which the back-scattered signals are correlated.

It was, however, demonstrated by simulations that incorrect estimates can result when searching the whole cross-correlation function for the maximum location. The problem can partly be solved by limiting the search to lie within the main lobe of the cross-correlation function. This has the penalty of limiting the maximum detectable velocity to the same as that for the autocorrelation approach.

Various methods for reducing the false maxima

problem and increasing the probability of correct detection were discussed. These techniques rely on either a temporal or spatial correlation between different estimates, and then deciding on the most probable estimate. The theoretical increase in probability of correct detection was derived, and the results of simple simulations were shown. For some of the more advanced spatial averaging techniques, a more elaborate simulation scheme than has been presented here, or measured data, would be necessary to quantify the improvement.

Acknowledgement—The author would like to thank Professor W. D. O'Brien and the anonymous reviewers for their help in preparing this paper.

REFERENCES

Bonnefous, O.; Pesqué, P.; Bernard, X. A new velocity estimator for color flow mapping. IEEE Ultrason. Symp. Proc. 855–860; 1986.

Bonnefous, O. Statistical analysis and the time correlation process applied to velocity measurement. IEEE Ultrason. Symp. Proc. 887–892; 1989.

Dotti, D.; Gatti, E.; Svelto, V.; Uggè, A.; Vidali, P. Blood flow measurements by ultrasound correlation techniques. Energia Nucleare 23:571–575; 1976.

Evans, D. H. Some aspects of the relationship between instantaneous volumetric blood flow and continuous wave Doppler recordings III. Ultrasound. Med. Biol. 8:617–623; 1982.

Evans, D. H.; McDicken, W. N.; Skidmore, R.; Woodcock, J. P. Doppler ultrasound, physics, instrumentation and clinical applications. New York: John Wiley & Sons; 1989.

Foster, S. G.; Embree, P. M.; O'Brien, W. D. Flow velocity profile via time-domain correlation: Error analysis and computer simulation. IEEE Trans. Ultrason. Ferroelectr. Freq. Contr. 37:164–175; 1990.

Hatle, L.; Angelsen, B. A. J. Doppler ultrasound in cardiology, physical principles and clinical applications. First edition. Philadelphia: Lea & Febiger; 1982.

Jensen, J. A. Stationary echo canceling in velocity estimation by time-domain cross-correlation. Accepted for publication in IEEE Trans. on Med. Imag.; 1993a.

Jensen, J. A. Artifacts in velocity estimation using ultrasound and cross-correlation. Accepted for publication in Med. and Bio. Eng. and Comp.; 1993b.

Kasai, C.; Namekawa, K.; Koyano, A.; Omoto, R. Real-time two-dimensional blood flow imaging using an autocorrelation technique. IEEE Trans. Sonics. Ultrason. 32:458–463; 1985.

Namekawa, K.; Kasai, C.; Tsukamoto, M.; Koyano, A. Realtime bloodflow imaging system utilizing autocorrelation techniques. In: Lerski, R. A.; Morley, P., ed; Ultrasound '82. New York: Pergamon Press; 1982; 203–208.

Womersley, J. R. Oscillatory motion of a viscous liquid in a thin-walled elastic tube. I: The linear approximation for long waves. Phil. Mag. 46:199–221; 1955.